Hot-Film and LDV Investigation of the Boundary Layer Transition on a Turbine Profile at Different Reynolds Numbers

DANIELE SIMONI, MARINA UBALDI, PIETRO ZUNINO
Department of Fluid Machines, Energy Systems and Transportation
University of Genova
Via Montallegro 1, I-16145 Genova
ITALY
daniele.simoni@unige.it, marina.ubaldi@unige.it, pietro.zunino@unige.it

Abstract: - An experimental investigation of the suction side boundary layer of a large scale turbine cascade has been performed to study the effect of Reynolds number on the boundary layer transition process at large ($1.6x10^6$) and moderate ($5.9x10^5$) Reynolds numbers.
The boundary layer development has been investigated by means of a two-component laser Doppler velocimeter. Time traces of the instantaneous velocities and boundary layer velocity and turbulence fields provide a physical insight of the different transition processes for the two Reynolds numbers.
Surface mounted hot-film gauges were used to measure the quantity $q\tau_w$, which is proportional to the wall shear stress. Statistical analysis of the instantaneous $q\tau_w$ data, including statistical moments, probability density function and intermittency function distributions, provides quantitative information on the state of advancement of the transition process at the two different Reynolds numbers.

Key-Words: - Boundary layer transition, Turbine profile, Hot-film probes, Wall shear stress, Intermittency detection technique, LDV measurements.

1 Introduction

Accurate numerical prediction of the transitional boundary layer on turbomachines blades is still a not completely resolved issue. Therefore, detailed experimental data specially produced for turbulence model assessment purpose are of primary importance for improving transition model predictive capabilities.

With this view an extensive database concerning the transitional boundary layer development at high Reynolds number (Re_{2c} =$1.6x10^6$) on the suction side of a gas turbine vane was experimentally produced by the authors [1]. The database, adopted as official test case by the ERCOFTAC Transition Modelling SIG10 and TRANSPRETURB (European Thematic Network on Implementation and Further Application of Refined Transition Prediction Methods for Turbomachinery), has been widely employed by research groups operating in turbulence and transition modelling [2-5].

With the aim of investigating the effect of Reynolds number on the blade boundary layer transition, new experiments have been recently performed on the same geometry at a lower Reynolds number Re_{2c} =$5.9x10^5$. Direct information on the boundary layer local state and its time-varying characteristics has been obtained from surface mounted hot-film gauges located in 29 measuring points distributed all along the profile suction side. The instantaneous hot-film outputs have been processed in order to determine a quantity $q\tau_w$ which is proportional to the wall shear stress.

The Reynolds number effects on boundary layer transition have been analysed in term of spatial distributions of the $q\tau_w$ statistical moments along the profile suction side The intermittency function, which describes in a quantitative way the transition process, has also been evaluated by means of a turbulent event detection technique based on the analysis of the probability density function of the instantaneous $q\tau_w$ data.

The suction side boundary layer at the two Reynolds numbers has been investigated in detail by means of a two-component Laser Doppler Velocimeter (LDV). Time traces of the instantaneous velocities, boundary layer velocity and turbulence fields illustrate the effects of the Reynolds number on the transition process.

2 Experimental Setup

2.1 Test facility and test conditions

The blade boundary layer development was surveyed on the blade suction side of a large-scale linear turbine cascade installed in the low-speed wind tunnel of DIMSET. The facility is a continuously operating variable speed wind tunnel with an open test section of 500x300 mm^2. A three-blade cascade with the largest possible blade chord was used so as to maximise measurement spatial resolution.

The blade profile is representative of a coolable hp gas turbine nozzle blade and is the same tested during an European project on time-varying wake flow characteristics on flat plates and turbine cascades [6-8]. The relevant geometrical characteristics of the cascade are: chord length c = 300 mm, pitch-to-chord ratio g/c = 0.7, blade aspect ratio h/c = 1, gauging angle β_2' = 19.2°. The profile velocity distribution is shown in Fig. 1.

The upstream turbulence level based on the streamwise velocity fluctuations and inlet velocity was 3.0 %. The integral length scale evaluated from the power density spectrum of the streamwise velocity [9] was 3.7% of the cascade chord length. These parameters were found nearly constant in the range of the Reynolds number of the present experiments (Re_{2c}= 5.9x10^5 to 1.6x10^6).

2.2 Hot-film instrumentation

The single-sensor hot-film element (Dantec 55R47) consists of a 0.1x0.9 mm thin nickel film applied by vapour deposition on a 50 μm thick polyimide substrate.

Due to analogy between heat and momentum transfer in boundary layers, the local instantaneous wall shear stress is related to the rate of heat transfer from the hot sensor to the fluid [10]:

$$\tau_w = k\left[\left(e^2 - A^2\right)/\Delta T\right]^3 \qquad (1)$$

where e is the instantaneous voltage and ΔT *i*s the temperature difference between sensor and fluid. As pointed out by several authors [11-15], useful information on the boundary layer transition and separation phenomena, as well as on its unsteady properties, can be obtained by a semi-quantitative analysis avoiding probe calibration. According to [12], eq. (1) can be approximated by

$$\tau_w \equiv k\left[\left(e^2 - e_0{}^2\right)/e_0{}^2\right]^3 \qquad (2)$$

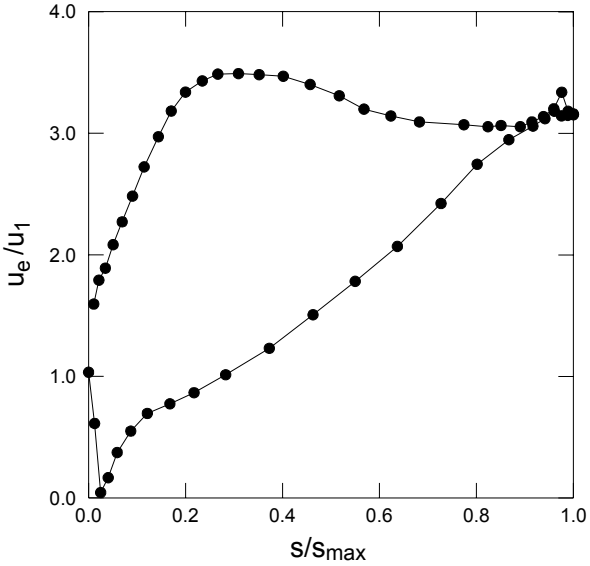

Figure 1. Profile velocity distribution

The quantity $\left[\left(e^2 - e_0{}^2\right)/e_0{}^2\right]^3$ is referred as instantaneous quasi wall shear stress $q\tau_w$.

2.3 Laser Doppler Instrumentation

A two-colour fibre optic LDV system with backscatter collection optics (Dantec Fiber Flow) was used for the present investigation. The light source is a 300 mW argon ion laser operating at 488 nm (blue) and 514.5 nm (green).

The probe consists of an optical transducer head of 60 mm diameter connected to the emitting optics and to the photomultipliers by means of optic fibres. The probe volume of 47 μm diameter and 0.4 mm length contains two sets of blue and green fringes (with spacing of 2.1 μm and 2.2 μm, respectively), which allow the simultaneous measurement of two velocity components in the plane perpendicular to the probe optical axis. A Bragg cell is used to apply a frequency shift (40 MHz) to one of each pair of beams, providing directional sensitivity and reducing angle bias for all velocity measurements. The signals from the photomultipliers are processed by two Enhanced Burst Spectrum Analysers.

2.4 Experiment Organisation

The location of the measuring points and their corresponding reference numbers are shown in Fig. 2.

2.4.1 Hot-film measurements

The gauge was glued on a 25 μm thick strip of acetate of length appropriate to avoid any surface

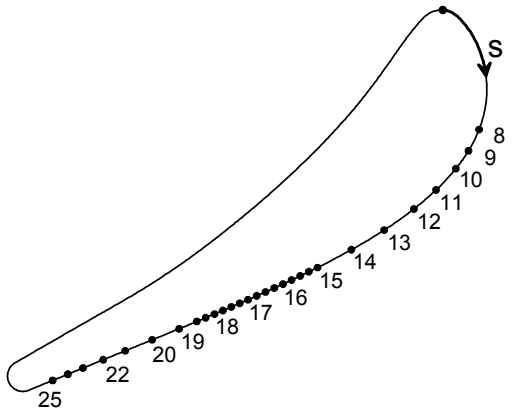

Figure 2. Blade profile and measuring positions

discontinuity near the sensor. The strip was fixed on the blade surface by means of a thin bi-adhesive tape and easily repositioned to investigate the whole blade surface. Measurements were performed for seven different Reynolds numbers ranging from Re_{2c}= 1.5x10^5 to 1.6x10^6.

The film element was connected to a constant-temperature hot-wire unit (Dantec 55M10, 55M17), which maintains the film at the selected temperature difference with respect to the fluid (60 °C). The system frequency response, deduced by a square wave test performed with the probe exposed to the flow, exceeds 20 kHz. An antialiasing low-pass filter with a cut-off frequency of 20 kHz was applied to the anemometer signal before it was sampled at a frequency of 50 kHz by means of a 12 bit A/D converter board.

For each measuring position, a total of 172032 data was taken. Probability density functions of the instantaneous quasi wall shear stress and statistical moments, including intermittency parameter, were evaluated for each measuring point.

2.4.2 LDV measurements

The probe volume was oriented with the larger dimension along the spanwise direction in order to have better spatial resolution in the wall normal direction. In order to measure simultaneously streamwise and normal velocities close to the blade surface, the optical axis was tilted towards the wall of about half the angle of the intersecting beams. The LDV probe was traversed using a three-axis computer controlled probe traversing system with a minimum linear translation step of 8 μm.

The boundary layer was surveyed by means of 31 traverses normal to the blade surface at midspan. The location of the boundary layer traverses and their corresponding reference numbers are shown in Fig. 2. Each boundary layer traverse is constituted by 34 measuring points. The distance between adjacent points was set at 25 μm in the region of the boundary layer close to the wall and was progressively increased in the outer part.

The measurements of the two velocity components were made in coincidence mode. Typical data rate was 10 kHz falling off to few kHz in the inner part of the boundary layer. For each measuring point 30000 samples were collected to obtain accurate statistical analysis. LDV data processing procedures are described in detail in [16].

2.5 Intermittency evaluation procedure

The hot-film signal presents a high sensitivity to the turbulent spots and one can try to discriminate turbulent and non-turbulent states by analyzing the power density function (pdf) of the $q\tau_w$ signal [17].

The objective of the method is to evaluate the intermittency Γ, defined as the portion of time during which the boundary layer is in turbulent state compared to the complete period of observation. It means that Γ is equal to 0 when the boundary layer is laminar and becomes 1 when the boundary layer is turbulent. The advancement of the transition process is therefore quantitatively represented by the variation of Γ along the profile.

The method has been implemented in the present work by means of a least squares fitting of the turbulent portion of the pdf:

$$P(x) = A_1 \exp\left[-\left(\frac{x - A_2}{A_3}\right)^2\right] \quad (3)$$

where A_1 amplitude, A_2 centre and A_3 width of the Gaussian fit are obtained using a non-linear least squares routine based on Levenberg-Marquardt method. The minimum value of $q\tau_w$ for the turbulent portion of the data record pdf, located in the valley between high and low shear portions, is defined iteratively in order to obtain the best fit.

The intermittency is calculated as

$$\Gamma = \int P(x)dx = A_1 A_3 \sqrt{\pi} \quad (4)$$

3 Results and Discussion

3.1 Hot-film measurements

In the present section the analysis of the effect of Reynolds number variation on transition, based on the $q\tau_w$ data, is presented.

3.1.1 $q\tau_w$ time traces and probability density functions

Figure 3 shows the evolution of the transition process at the largest Reynolds number (Re_{2c}= 1.6x10^6). The time trace at position 12 indicates a laminar condition with low $q\tau_w$ mean values and absence of fluctuations (laminar state). The corresponding probability density function (pdf) is a very sharp nearly gaussian distribution, typical of a laminar state.

At station 14 the transition starts to take place. The pdf assumes a double peak structure typical of the transition process. At this stage the boundary layer is prevalently laminar as shown by the stronger peak in pdf at lower $q\tau_w$ and a small but clearly visible turbulent contribution at larger $q\tau_w$.

Station 15 is exactly at the transition point (turbulent state for 50% of time). The boundary layer switches between laminar and turbulent states. The $q\tau_w$ oscillates between low (laminar) and large (turbulent) values.

At station 15.5 the transition process is advanced (turbulent state for more than 50% of the time). The probability density function presents a tail on the left side due to the negative spikes associated with the still existing but more rare laminar conditions.

Finally at station 18, the boundary layer is in a fully turbulent state characterized by turbulent fluctuations. Turbulent fluctuations have a larger frequency and a lower amplitude compared to the $q\tau_w$ fluctuations associated with the change of state of the boundary layer during transition. In the turbulent condition the pdf is a large frequency range gaussian distribution.

At the lower Reynolds number Re_{2c}= 5.9x10^5 (Fig. 4) the transition process takes place in a different way. At station 14 the boundary layer is in a laminar, near separation condition characterized by very low values of $q\tau_w$.

At station 16 the transition process, probably triggered by the incipient separation condition, takes place very rapidly with extended turbulent spots. At station 16.5 the transition is well advanced with a nearly 50% of the time of turbulent state.

At station 18 the boundary layer is already become turbulent. Compared with the case at largest Reynolds number (Re_{2c}= 1.6x10^5), here (Re_{2c}= 5.9x10^5) the transition process initiates later, but it is more rapid and terminates approximately at the same position of the large Reynolds number condition.

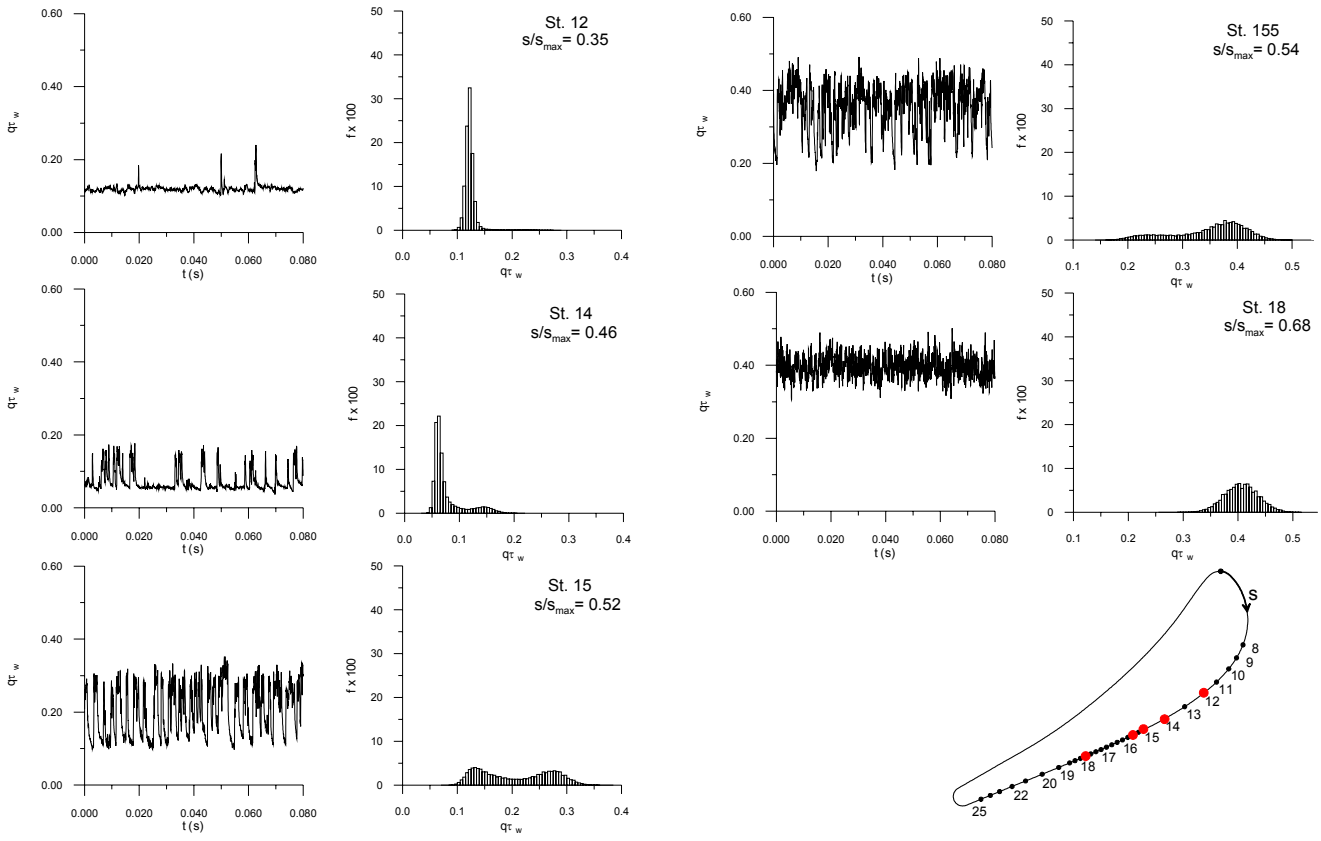

Figure 3. $q\tau_w$ time traces and probability density functions Re_{2c} =1.6 x 10^6

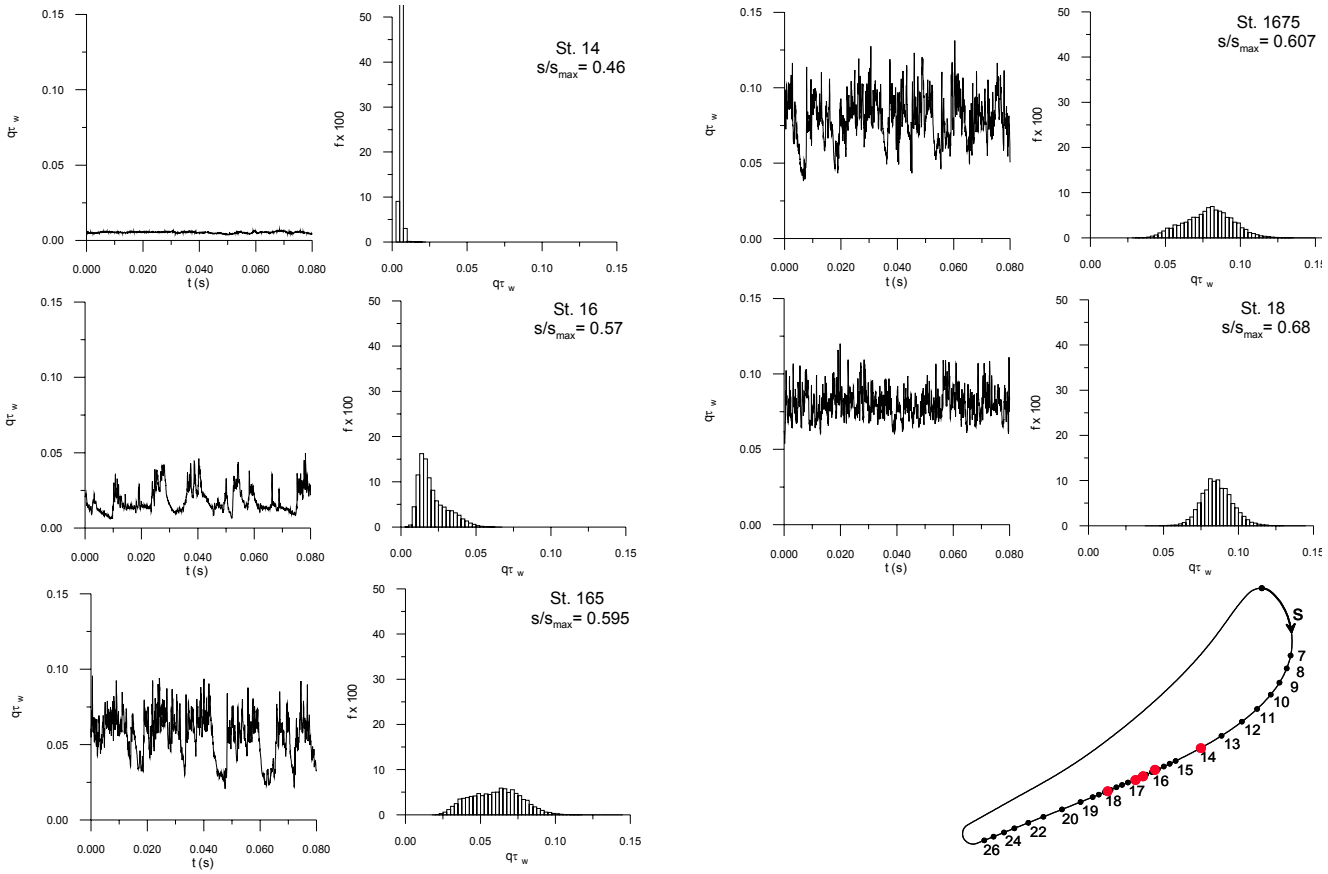

Figure 4. $q\tau_w$ **time traces and probability density functions** Re_{2c} **=5.9 x** 10^5

3.1.2 $q\tau_w$ statistical moments

Figure 5 shows the distributions along the blade suction side surface of the time averaged $q\tau_w$ together with the variance and skewness coefficients of the $q\tau_w$ fluctuations for the two Reynolds numbers investigated Re_{2c} = 590000 and 1600000.

Characteristic positions associated with the

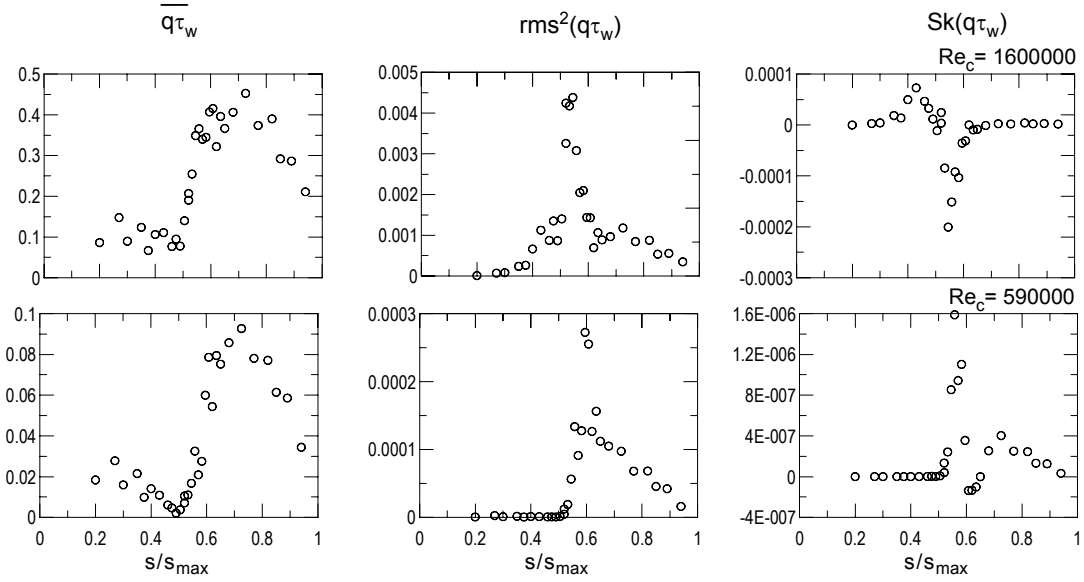

Figure 5. Distributions of $q\tau_w$ **statistical moments for** Re_{2c}**= 1.5x**10^5 **to 1.6x**10^6

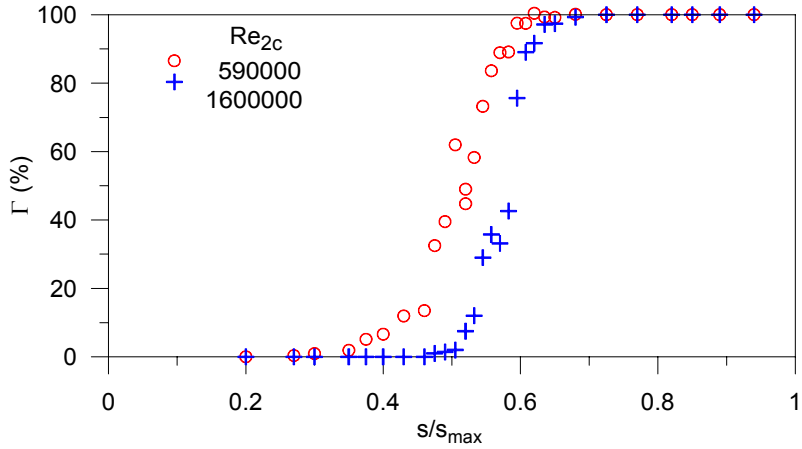

Figure 6. Distributions of the intermittency function

transition process can be identified from these distributions. The start of transition can be located at the point where the variance starts to increase and the skewness moves from zero to positive values. This point is in the region where $\overline{q\tau_w}$ is low but has not yet reached its relative minimum. The transition point can be defined by the maximum of the variance distribution, which corresponds to a region of large positive gradient of $\overline{q\tau_w}$ and to the position where the skewness coefficient is changing sign decreasing from the positive region to the negative one. Finally the end of transition can be identified by the variance return to a nearly constant value and the skewness return to zero.

At Re_{2c}=590000 $\overline{q\tau_w}$ presents a clear relative minimum which attains the null value at s/s_{max}=0.5, exactly where variance moves steeply from zero and skewness becomes suddenly positive. Probably this is a critical condition where both laminar separation and transition conditions occur at the same time.

The acceleration of the transition process is the most important effect of the Reynolds number increase.

A more quantitative information on the transition onset and completion is given by the intermittency parameter that has been evaluated from the instantaneous hot-film signals by means of the pdf based detection algorithm briefly described in the subsection 2.5.

3.1.3 Intermittency function

The intermittency function Γ has been evaluated using eq. (4) for all the measuring points. The intermittency function distribution is reported in Fig. 6 for Re_{2c} = 590000 and Re_{2c} = 1600000.

Figure 6 clearly shows that the start of transition is located at s/s_{max}=0.3 for Re_{2c} = 1600000 and at s/s_{max} = 0.5 for Re_{2c} = 590000. The end of transition is located at about s/s_{max}=0.6 and s/s_{max}=0.65, respectively. This confirms a longer and smooth transition process for the higher Reynolds number and a sudden and rapid transition process, probably triggered by an incipient boundary layer separation, for the lower Reynolds number.

3.2 LDV measurements

3.2.1 Instantaneous velocities within the boundary layer

To gain information on the flow time structure, the time traces of instantaneous velocity within the boundary layer have been investigated. The maximum obtainable data density, defined as the ratio between the turbulence integral time scale T_i and the mean valid data interarrival time Δt_s, is in the present investigation of the order of 20, a value large enough to reveal the general features of the time structure of the flow. Figure 7 reports the time traces of the velocity detected in 3 locations: St14 s/s_{max}=0.46, St16 s/s_{max}=0.57, St19 s/s_{max}=0.77, characteristic of laminar, transitional and turbulent conditions, respectively. For each station the distributions are given for three values of the non dimensional normal distance y^+.

At station 14 the boundary layer is still in laminar state, as shown by the very low velocity

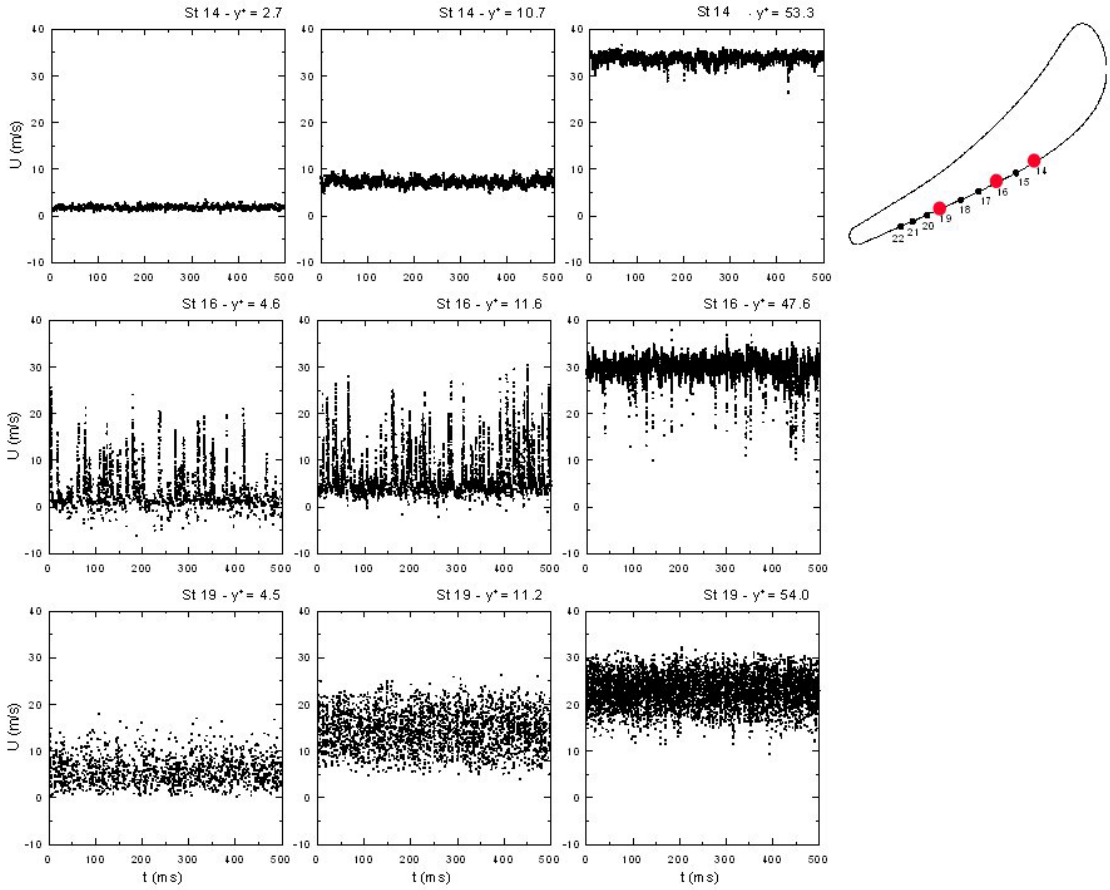

Figure 7. Instantaneous velocities within the boundary layer Re_{2c} =5.9 x 10^5

variations of the time traces at the different distances from the wall.

The most striking feature of the velocity traces of station 16 is the presence of not so frequent one-side velocity fluctuations, which determines the intermittent switching of the velocity from laminar to turbulent conditions. At y^+= 4.6 time trace shows also some negative velocity values, clearly indicating the tendency of the boundary layer to separate. At station 19, the turbulence structure is characterised by higher frequency, large two-side velocity fluctuations, typical of a turbulent boundary layer.

3.2.2 Boundary layer velocity and turbulence fields

The LDV instantaneous data have been weighted averaged to obtain boundary layer velocity and turbulence profiles and, considering all the profiles together, also the boundary layer velocity and turbulence fields.

The colour plots of Figs. 8 an 9 provide an overall view of the boundary layer development and the associated turbulence from laminar to turbulent state.

Figure 8 refers to case of higher Reynolds number (Re_{2c} =5.9x10^5)and Figure 9 reports the results at lower Reynolds number (Re_{2c} =1.6x10^6): on the top of both figures the colour plot of the streamwise velocity with the vector plots superimposed, on the bottom the rms of the streamwise velocity.

Starting from Fig. 8 and from the steamwise velocity fields, one can observe the free stream flow acceleration up to the region of maximum velocity and the subsequent region of diffusion. The boundary layer is thin in the accelerated region, the transition takes place in the decelerated region and finally the velocity field shows the increase of the turbulent boundary layer after s/s_{max}=0.6.

Low rms values in the forward part of the rms field (left hand side) confirm the laminar boundary layer nature at the beginning. However, before the transition process takes place, the rms starts to increase in the near wall region indicating an early beginning of instability at largest Reynolds number, which precedes the transition process. The transition

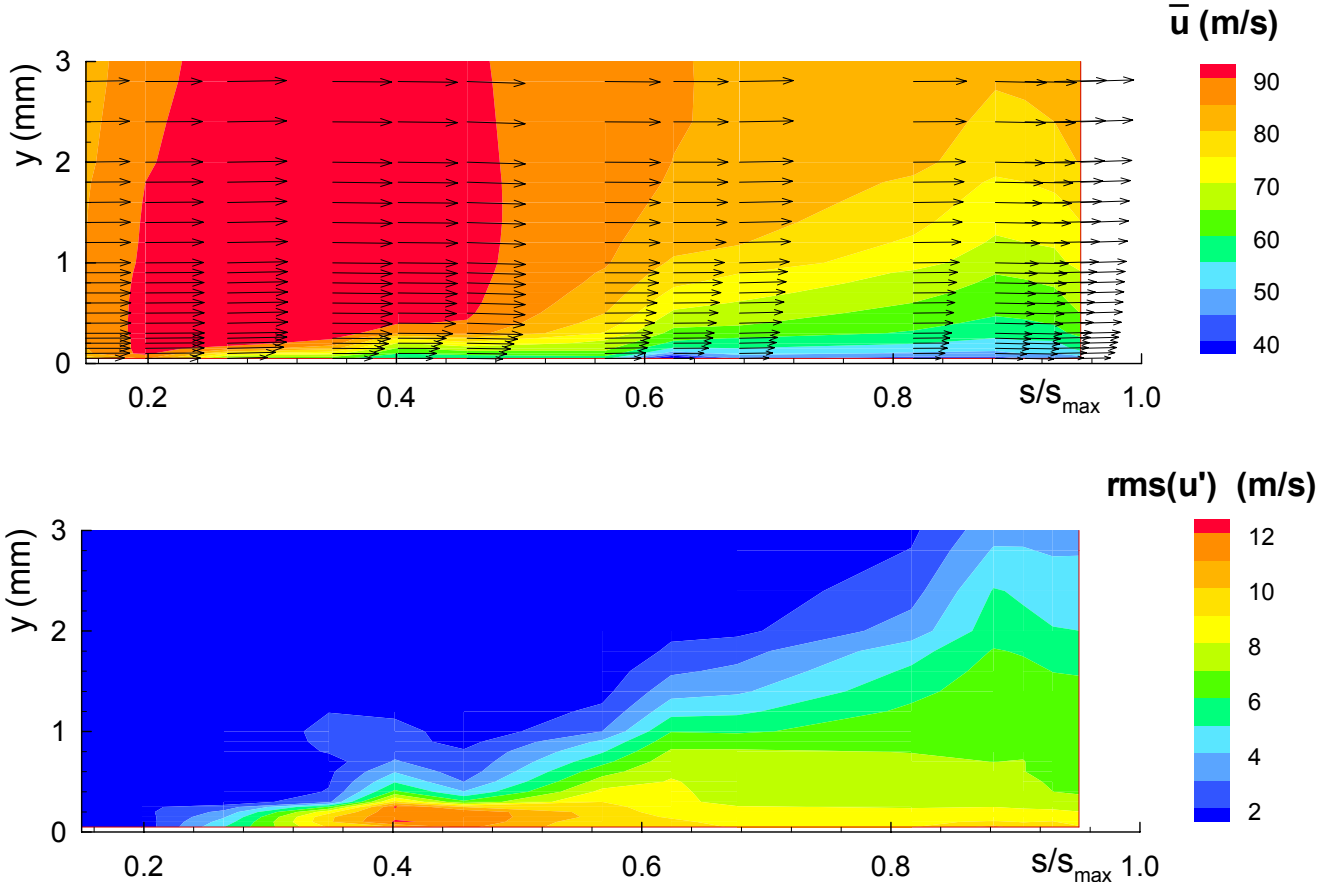

Figure 8. Boundary layer velocity and turbulence fields Re_{2c} =1.6 x 10^6

process takes place approximately from s/s_{max}=0.3 to 0.6 with a significant increase of the rms of the velocity in the region near the wall, due to the intermittent nature of the phenomenon with alternation of laminar and turbulent states.

Finally the rear part of the rms field shows a streamwise turbulence distributions which is typical of the turbulent boundary layer state.

In the case of lower Reynolds number the velocity and rms fields (Fig. 9) indicate a different development of the transition process.

In the forward part of the profile the boundary layer thickens significantly, because the start of transition is delayed due to the effect of reduced Reynolds number. The laminar boundary layer develops up to about s/s_{max}=0.53 with a progressive reduction of the friction velocity and consequent risk increase of separation. The occurrence of separation before transition is correlated to the profile Reynolfd number and flow freestream turbulence intensity (e.i.[18]). The phenomenon has been recently investigated also with numerical simulations [19].

At s/s_{max}= 0.53 the laminar boundary layer stays simultaneously in an incipient state of separation and on the verge of transition (Reynolds number based on momentum thickness Re_{ϑ} =390). Therefore the transition takes place vigorously in a short spatial extension (from s/s_{max}= 0.55 to s/s_{max}= 0.65) as shown by the strong peak of rms values located separately from the wall. From s/s_{max}= 0.65 onwards the plots show a typical boundary layer development in terms of velocity and turbulence fields, as expected much extended compared to the case at larger Reynolds number.

4 Conclusions

Surface mounted hot-film instrumentation was employed to investigate the effect of Reynolds number on the boundary layer transition process in a large scale turbine cascade. Hot-film investigation was complemented with local boundary layer LDV measurements.

The most relevant conclusions of the present investigation are as follows:

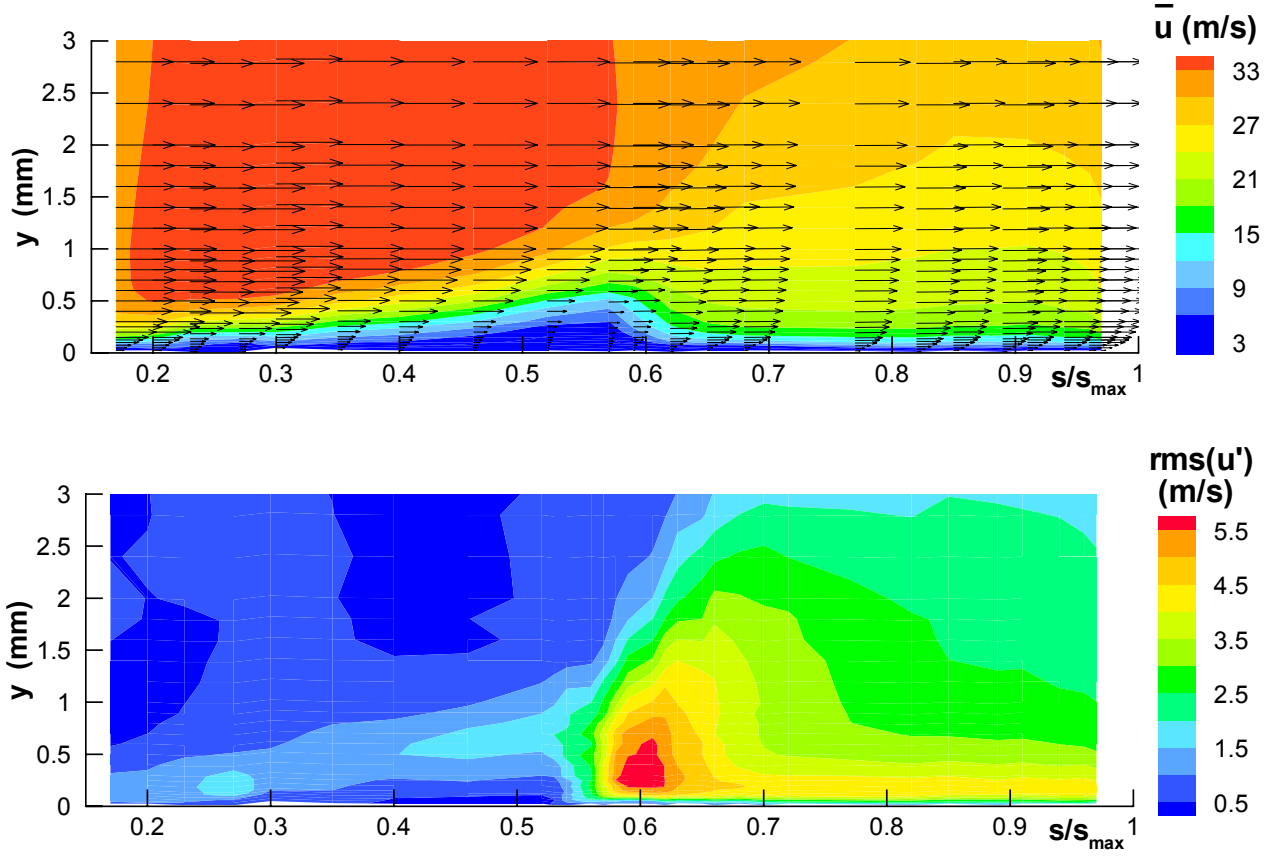

Figure 9. Boundary layer velocity and turbulence fields Re_{2c} =5.9 x 10^5

- Both distributions of $q\tau_w$ and intermittency function show that at Reynolds number Re_{2c} = 1600000 the transition process is long and gradually takes place from s/s_{max} =0.30 until s/s_{max} =0.6. At a moderate Reynolds number Re_{2c}=590000 the transition starts suddenly at s/s_{max} =0.5, probably triggered by an incipient boundary layer separation, and it is rapidly completed at s/s_{max} =0.65.
- Velocity and turbulence colour plots document the boundary layer development down to the near wall region. During transition the streamwise velocity fluctuations are strongly amplified especially in the near wall region were rms(u') attains values which are much larger than in the turbulent regime.
- Time traces of the instantaneous velocity taken at different distances from the blade surface show clearly the intermittent switches of the velocity from laminar to turbulent conditions taking place in the near wall regions and indicate that at moderate Reynolds number the boundary layer has a tendency to separate before transition.
- Accuracy and spatial resolution of measurements, and completeness of results make the present data a test case suitable for turbulence and transition models used in numerical prediction of boundary layer transition.

Nomenclature

c	blade chord length
e	hot-film voltage
e_0	hot-film voltage at zero flow condition
$q\tau_w$	quasi wall shear stress
Re_{2c}	Reynolds number based on cascade outlet velocity and chord length = $u_2 c/\nu$
Sk	skewness coefficient
s	surface distance measured from leading edge
s_{max}	surface length from leading to trailing edge
u	instantaneous velocity components in streamwise direction
u'	velocity fluctuations in streamwise directions
u_e	local free-stream velocity

u_1 cascade inlet velocity
u_2 cascade outlet velocity
y^+ dimensionless distance from the blade surface = yu_τ / ν
Γ intermittency
ν kinematic viscosity
ρ fluid density
τ_w wall shear stress

Overbar

$\overline{}$ time averaged

References:

[1] M. Ubaldi, P. Zunino, U. Campora, A. Ghiglione, Detailed velocity and turbulence measurements of the profile boundary layer in a large scale turbine cascade, ASME Paper No. 96-GT-42, 1996.

[2] W.L. Chen, M.A. Leschziner, Modeling turbomachine-blade flows with non-linear eddy-viscosity models and second-moment closure, *Third European Conference on Turbomachinery - Volume A, IMechE Conference Transaction*, 1999.

[3] F. Magagnato, Unsteady flow past a turbine blade using non-linear two-equation turbulence models, *Third European Conference on Turbomachinery - Volume A, IMechE Conference Transaction,* 1999.

[4] F.K. O'Donnell, M.R.D. Davies, Turbine Blade Entropy Generation Rate. Part II: The Measured Loss, ASME Paper No. 2000-GT-266, 2000.

[5] F.R. Menter, T. Esch, S. Kubacki, Transition Modelling based on local variables, *5th Int. Symp. on Engineering Turbulence Modelling and Measurements*, Mallorca, Spain, 2002.

[6] C. H. Sieverding, G. Cicatelli., J.M. Desse, M-Meinke, P. Zunino, *Experimental and Numerical Investigation of Time Varying Wakes behind Turbine Blades,* Vieweg, Braunschweig, 1999.

[7] M. Ubaldi, P. Zunino, Transition and Loss Generation in the Profile Boundary Layer of a Turbine Blade, *WSEAS Transactions on Fluid Mechanics*, Vol. 1, 2006, pp. 779-784.

[8] D. Simoni, M. Ubaldi., P. Zunino, Von Karman Vortices Formation at the Trailing Edge of a Turbine Blade, *WSEAS Transactions on Fluid Mechanics*, Issue 4, Volume 3, October 2008.

[9] T. Cebeci, A.M.O. Smith, *Analysis of Turbulent Boundary Layers*, Academic Press, New York, 1974.

[10] B.J Bellhouse, D.L. Schultz, Determination of mean and dynamic skin friction, separation and transition in low-speed flow with a thin-film heated element, *J. Fluid Mech.,* Vol. 24, No. 2, 1966, pp. 379-400.

[11] M. L. G. Oldfield, R. Kiock,, A. T. Holmes, C. G. Graham, Boundary Layer Studies on Highly Loaded Cascades using Heated Thin Films and a Traversing Probe, *ASME Journal of Engineering for Power,* Vol. 103, 1981, pp. 237-246.

[12] H.P. Hodson, Boundary-Layer Transition and Separation Near the Leading Edge of a High-Speed Turbine Blade, *ASME Journal of Engineering for Gas Turbines and Power*, Vol. 107, 1985, pp.127-134.

[13] P. Pucher, R. Göhl, Experimental Investigation of Boundary Layer Separation With Heated Thin-Film Sensors, *ASME Journal of Turbomachinery*, Vol. 109, 1987, pp. 303-309.

[14] J. Hourmouziadis, F. Buckl, P. Bergmann, The Development of the Profile Boundary Layer in a Turbine Environment, *ASME Journal of Turbomachinery*, Vol. 109, 1987, pp. 286-295.

[15] D. E. Halstead, et al., Boundary Layer Development in Axial Compressors and Turbines-Part 1 of 4: Composite Picture, ASME Paper No. 95-GT-461, 1995.

[16] U. Campora, F. Pittaluga, M. Ubaldi, P. Zunino, A Detailed Investigation of the Transitional Boundary Layer on the Suction Side of a Turbine Blade, *XV Symposium on Measuring Techniques in Transonic and Supersonic Flow in Cascades and Turbomachines*, Firenze, Italy, 2000.

[17] S.P. Schneider, Improved methods for measuring laminar–turbulent intermittency in boundary layers, *Experiments in Fluids*, Vol. 18, 1995, pp. 370-375.

[18] R. E. Mayle, The Role of Laminar-Turbulent Transition in Gas Turbine Engines, *ASME Journal of Turbomachinery*, Vol. 113, 1991, pp. 509-531.

[19] V. S. Djanali, K.C. Wong, S.W. Armfield, Numerical Simulations of Transition and Separation on a Small Turbine Cascade, *WSEAS Transactions on Fluid Mechanics*, Vol. 1, 2006, pp. 879-884.